

## Emission property of Y<sub>2</sub>O<sub>3</sub>-doped Mo secondary emitter

WANG Jin-shu(王金淑), LIU Wei(刘伟), LI Hong-yi(李洪义), GAO Fei(高非),  
REN Zhi-yuan(任志远), ZHOU Mei-ling(周美玲)

School of Materials Science and Engineering, Beijing University of Technology, Beijing 100022, China

Received 10 November 2008; accepted 29 April 2009

**Abstract:** Y<sub>2</sub>O<sub>3</sub>-doped Mo secondary emitters were prepared by liquid-liquid doping and solid-solid doping, respectively. The back-scattered scanning observation result indicates that the emitter prepared by liquid-liquid doping has fine microstructure whereas that prepared by solid-solid doping has large grain size. Y<sub>2</sub>O<sub>3</sub>-doped Mo emitter with small grain size prepared by liquid-liquid doping exhibits high emission property, i.e., the secondary electron yield can get to 5.24, about 1.7 times that prepared by solid-solid doping. Moreover, Y<sub>2</sub>O<sub>3</sub>-doped Mo emitter exhibits the best emission performance among La<sub>2</sub>O<sub>3</sub>-doped Mo, Y<sub>2</sub>O<sub>3</sub>-doped Mo, Gd<sub>2</sub>O<sub>3</sub>-doped Mo and Ce<sub>2</sub>O<sub>3</sub>-doped Mo emitters due to the largest penetration depth of primary electrons and escape depth of secondary electrons in this emitter. The secondary emission of the emitter with small grain size can be explained by reflection emission model and transmission emission model, whereas only transmission emission exists in the emitter with large grain size.

**Key words:** Y<sub>2</sub>O<sub>3</sub>-doped Mo; powder metallurgy; emission property; microstructure

## 1 Introduction

Secondary emission has been used in many fields stimulated by the development of imaging of surface topography, plasma display panels and magnetrons[1–2]. And magnetrons have been used in the area of broadcasting, communication and aviation industry due to their many advantages including high efficiency, low cost and low voltage[3–4]. Being the heart of electron tubes and magnetrons, the emitters play an important role in those devices. At present, Ba-W emitters[5], oxide emitters and ThO<sub>2</sub>-W emitters, especially Ba-W emitters, are commonly used in the high power magnetrons. However, Ba-W emitters are hard to be made and sensitive to the atmosphere during preparation and treatment. The oxide emitters, like thick film emitters, have higher secondary emission yields, but possess bad anti-ion bombardment property and short life. ThO<sub>2</sub>-W emitters face problems of high working temperature and radioactivity of ThO<sub>2</sub>. It was found that rare earth oxide (RE<sub>2</sub>O<sub>3</sub>)-doped Mo could be used as a new type of emitter material for magnetrons[6–10]. The secondary

emission yield of about 3.24 could be obtained after the emitter was activated at the temperature as high as 1 600 °C[6]. In the present study, we intend to improve the secondary emission yield and decrease the activation temperature since high temperature activation needs to use high temperature emitter assembly materials in the magnetron and causes high energy cost.

## 2 Experimental

### 2.1 Preparation of Y<sub>2</sub>O<sub>3</sub>-doped Mo sample

Y<sub>2</sub>O<sub>3</sub>-doped Mo powders were prepared by liquid-liquid doping using a sol-gel technique. Yttrium nitrate and ammonia molybdate were used as raw materials. The content of Y<sub>2</sub>O<sub>3</sub> was 30% in mass fraction. The doped molybdenum oxide powders were reduced into metallic molybdenum powders by dry hydrogen at high temperature. Then, the powders were pressed into a pellet and sintered by spark plasma sintering (SPS) at 1 500 °C for 3 min to form Y<sub>2</sub>O<sub>3</sub>-doped Mo bar. For comparison, a raw powder material of Y<sub>2</sub>O<sub>3</sub> containing 95% Y<sub>2</sub>O<sub>3</sub> and 5% impurities was used and mixed with molybdenum powder.

## 2.2 Measurement of emission properties

The sintered  $Y_2O_3$ -doped Mo bars were machined into thin flakes ( $d10\text{ mm}\times 2\text{ mm}$ ) and connected with molybdenum sleeves by laser welding. The emitter assembly was heat treated at  $1\ 450\text{ }^\circ\text{C}$  under the flow of hydrogen. Emission properties of the emitters activated at  $1\ 400\text{ }^\circ\text{C}$  were tested in a close-spaced diode configuration in an ultra high vacuum (UHV) system and a Mo-cylinder with a water-cooled copper anode. A computer-controlled automatic emission testing instrument, which had been described in Ref.[6], was applied for the measurements. The secondary emission properties were measured at  $600\text{ }^\circ\text{C}$  in order to avoid the influence of the thermionic emission.

## 2.3 Observation of microstructure and element analysis for surface of sintered materials

The thermal analysis was carried out on an STA-449-Jupiter thermal analysis apparatus. The microstructure was observed with Hitachi S-3500N scanning electron microscope. In-situ AES analyses were carried out with a VG MICROLAB MK-II system.

## 3 Results and discussion

It was found in our previous work that the surface of  $La_2O_3$ -doped Mo emitter was covered by a  $La_2O_3$  layer[6]. The secondary emission process includes the secondary electrons generating (the inner electrons getting energy from the primary electrons), transporting to the surface, overcoming the surface barrier potential and escaping from the surface. Therefore, the secondary emission is related to this  $RE_2O_3$  layer.  $RE_2O_3$  is a kind of insulator at room temperature. All the secondary electrons in an insulator originate from the filled valence band deep below the conduction band[11]. When the primary electrons collide with  $RE_2O_3$ -doped Mo emitter, supposing that these electrons travel in a straight-line path, these electrons will transfer their kinetic energy to internally generated secondary electrons. As the primary electrons lose their initial energy, the production of secondary electrons reaches its maximum near the end of the primary electrons movement paths. Therefore, the internal secondary electrons generated exist in this primary range. The penetration depth of primary electrons and the escape depth of secondary electrons could be calculated by the following expressions presented by YOUNG[12] and DEKKER[13], respectively:

$$R = \frac{1.15 \times 10^2 E_p^{1.35}}{\rho} \quad (1)$$

where  $R$  is the penetration depth (nm);  $E_p$  is the primary

electron energy (keV); and  $\rho$  is the density of the materials( $\text{g}/\text{cm}^3$ );

$$\chi_s = \frac{50.4 E_{pm}^{1.35}}{\rho} \quad (2)$$

where  $\chi_s$  is the escape depth and  $E_{pm}$  is the primary electron energy at the maximum secondary emission yield. Eqs.(1) and (2) indicate that the lower the density of  $RE_2O_3$ , the larger the penetration depth of primary electrons or the escape depth of secondary electrons. The larger the penetration depth, the more the number of electrons in the emitter which could get the energy from the primary electrons, namely, the more the number of secondary electrons. So,  $RE_2O_3$  with lower density should have better secondary emission property. Taking the cost and density of raw materials into account,  $La_2O_3$ ,  $Y_2O_3$ ,  $CeO_2$  and  $Gd_2O_3$  were chosen as the starting materials. Fig.1 shows the penetration depth and escape depth for four  $RE_2O_3$  and  $ThO_2$  layers (an important composition of  $ThO_2$ -W emitter used in some magnetrons) covered on the related  $RE_2O_3$ -doped Mo emitters and  $ThO_2$ -W emitter. The densities of different oxides were obtained in Ref.[14]. It could be seen that

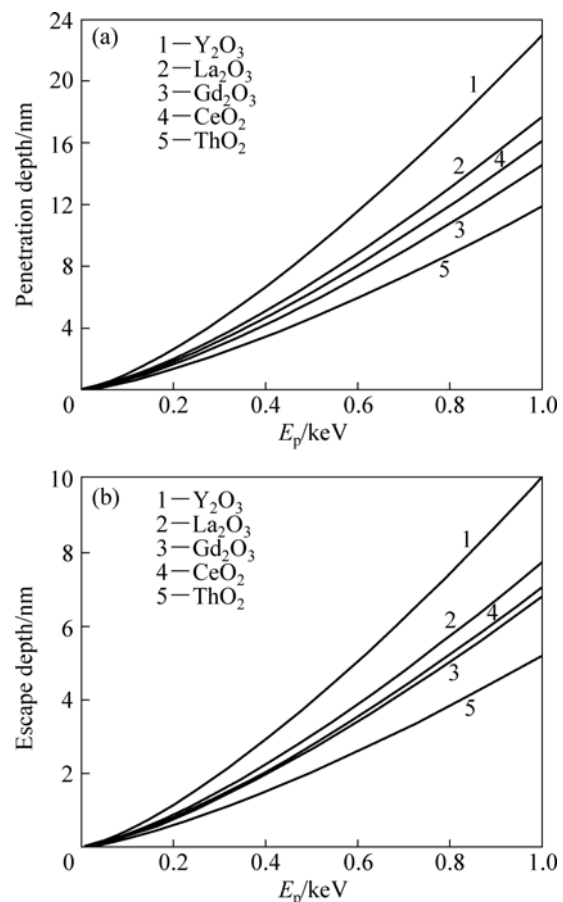


**Fig.1** Curves of penetration depth of primary electrons (a) and escape depth (b) of internal secondary electrons in different oxides as function of primary electron energy

compared with  $\text{ThO}_2$ , electrons with larger penetration depth and escape depth could be obtained for  $\text{RE}_2\text{O}_3$ .

The emission properties of these four kinds of  $\text{RE}_2\text{O}_3$ -doped Mo emitters were measured and results are shown in Fig.2. It is also found that  $\text{Y}_2\text{O}_3$ -doped Mo exhibits the highest secondary emission property. The maximum secondary emission yield ( $\delta_m$ ) could get to 5.24 whereas  $\text{La}_2\text{O}_3$ -doped Mo had the lowest one of 2.67. Our former report showed that  $\text{La}_2\text{O}_3$ -Mo prepared by solid-liquid doping method could provide the secondary emission yields of 2.66 and 2.01 after the emitters were activated at 1 600 °C and 1 400 °C, respectively. We notice that this emitter could provide the same secondary emission property after being activated at 1 400 °C as the former emitter was activated at 1 600 °C, indicating the improvement of the secondary emission property.  $\text{Y}_2\text{O}_3$  has the largest penetration depth and escape depth among all  $\text{RE}_2\text{O}_3$  samples. That is why  $\text{Y}_2\text{O}_3$ -doped Mo exhibits the best secondary emission property. The secondary emission property of the emitters is consistent with the penetration depth and escape depth of related  $\text{RE}_2\text{O}_3$  except for  $\text{La}_2\text{O}_3$ -doped Mo emitter.

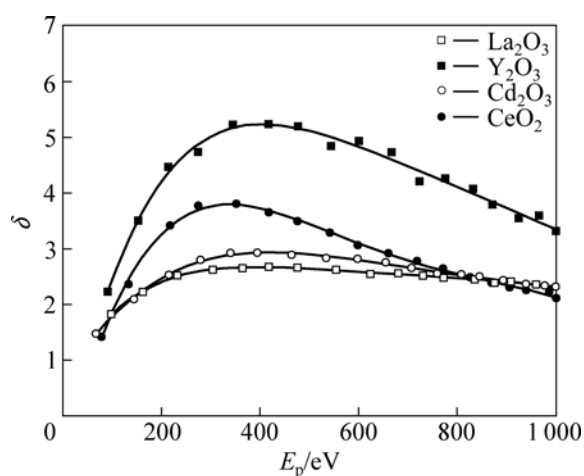


Fig.2  $\delta$ — $E_p$  curves of different  $\text{RE}_2\text{O}_3$ -Mo emitters

Fig.3 shows the microstructure of machined surface of  $\text{La}_2\text{O}_3$ -doped Mo and  $\text{Y}_2\text{O}_3$ -doped Mo emitters. It could be seen that many cracks appeared at  $\text{La}_2\text{O}_3$  part and along the boundaries between  $\text{La}_2\text{O}_3$  and Mo whereas it is hard to distinguish  $\text{Y}_2\text{O}_3$  and Mo grains. These results indicate that  $\text{La}_2\text{O}_3$  is easy to aggregate and the volume of  $\text{La}_2\text{O}_3$  increases probably due to the formation of other lanthanum compounds. It is well known that it is easy for  $\text{La}_2\text{O}_3$  to absorb water and gas to form other lanthanum compounds, which will lead to the volume increase of  $\text{La}_2\text{O}_3$ , resulting in the cracks on the emitter surface and the low secondary emission property of the emitter.

It is well known that metal molybdenum has a lot of

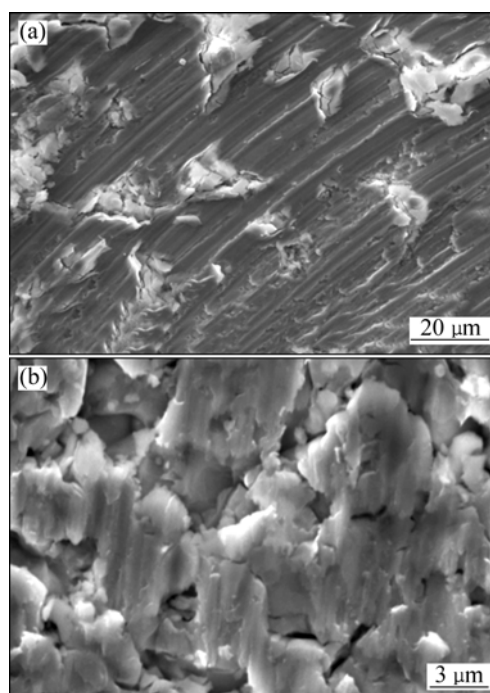


Fig.3 SEM images of machined surface of  $\text{La}_2\text{O}_3$ -Mo emitter (a) and  $\text{Y}_2\text{O}_3$ -Mo emitter (b)

free electrons. The penetration depth of primary electrons and escape depth of internal secondary electrons are small due to the huge collisions between free electrons of molybdenum and primary electrons, free electrons and internal secondary electrons, respectively, and thus molybdenum has a low secondary electron yield of 1.4[15]. There are few free electrons in insulator  $\text{RE}_2\text{O}_3$ . The energy loss of the secondary electrons in these rare earth oxides is low because of the decrease in the collisions between secondary electrons and free electrons. The secondary electrons mainly come from  $\text{RE}_2\text{O}_3$ . Supposing that  $\text{Y}_2\text{O}_3$  and Mo grains distribute alternately and  $\text{Y}_2\text{O}_3$  grain has a width of  $a$ , the energy of the primary electrons as a function of penetration depth has been calculated under the assumption that  $\text{Y}_2\text{O}_3$  surface is bombarded by an electron beam with an area of  $10 \text{ nm} \times 10 \text{ nm}$  and composed of 2 000 electrons by applying Monte Carlo method. In the magnetron practical application, the primary electrons with high energy bombard the emitter surface. Fig.4 shows the energy distributions of primary electrons in  $\text{Y}_2\text{O}_3$  with different width under 20 keV electron bombardment, where the shade of color indicates the variation of incidence electron energy. As shown in Fig.4, the electron energy decreases with increasing the width. The primary (incidence) electrons lose energy through collisions with electrons in the bulk materials. When the incidence electrons lose 95% of their energy, primary electrons travel to the end of their journey. The depth for the primary electrons traveling in the bulk materials

could be taken as the penetration depth. The penetration depth of electrons is 2 600 nm when  $Y_2O_3$  has a larger width of 4 000 nm(see Fig.4(a)), indicating that the secondary electrons are produced in  $Y_2O_3$  and thus the secondary emission mainly occurs in  $Y_2O_3$ . This emission could be called as reflection emission. When an insulator surface is bombarded with an electron beam, the surface is positively charged in the region of  $E_p$  where  $\delta$  is larger than 1. As a result, it is expected that some of the secondary electrons are pulled back to the surface by the positive holes, decreasing the magnitude of  $\delta$ . Therefore, the replenishment of electrons to the positive holes generated upon the incidence of primary electrons inside the  $Y_2O_3$ -doped Mo materials becomes very important. The conductivity of  $Y_2O_3$  is only 0.28 S/m at 600 °C, indicating that the replenishment of electrons from Mo to the holes is difficult since  $Y_2O_3$  is an excellent insulator. So, it is difficult to provide continuous emission. Decreasing width of  $Y_2O_3$  from 4 000 nm to 2 000, 1 000 and 500 nm, more and more incidence electrons will get into molybdenum grain to excite electrons in molybdenum. The internal secondary electrons produced in molybdenum get back to  $Y_2O_3$  grain to excite the electrons in the valence band of  $Y_2O_3$  when these internal secondary electrons have the energy larger than the bandgap energy  $E_g$  of  $Y_2O_3$ . Otherwise,

they will move to the emitter surface when the energy of the internal electrons is low. This kind of emission could be called as transmission emission. In such cases, two kinds of emissions, reflection emission formed by the secondary electrons produced by primary electrons and transmission emission formed by the secondary electrons in  $Y_2O_3$  excited by the internal secondary electrons produced in molybdenum, exist in the emitter. In addition, the positive charging effect of  $Y_2O_3$  layer, leading to a partial recapture of the secondary electrons generated on the surface, becomes reduced due to the easier flow of electrons from Mo to  $RE_2O_3$ . As a result, the secondary electrons can easily move away from the surface to vacuum at this stage with the decrease in the particle size of  $Y_2O_3$ .

Fig.5 shows the SEM images of  $Y_2O_3$ -doped Mo emitters prepared by mechanical mixing of  $Y_2O_3$  and Mo (we called as solid-solid doping) and liquid-liquid doping (two kinds of water soluble compounds of rare earth nitrite and ammonia molybdate were used as raw materials), respectively. The sample prepared by mechanical mixing method has fine microstructure whereas the sample prepared by liquid-liquid doping method has small grain size. The emitter prepared by solid-solid doping has the relatively low secondary emission property, i.e., the maximum secondary electron

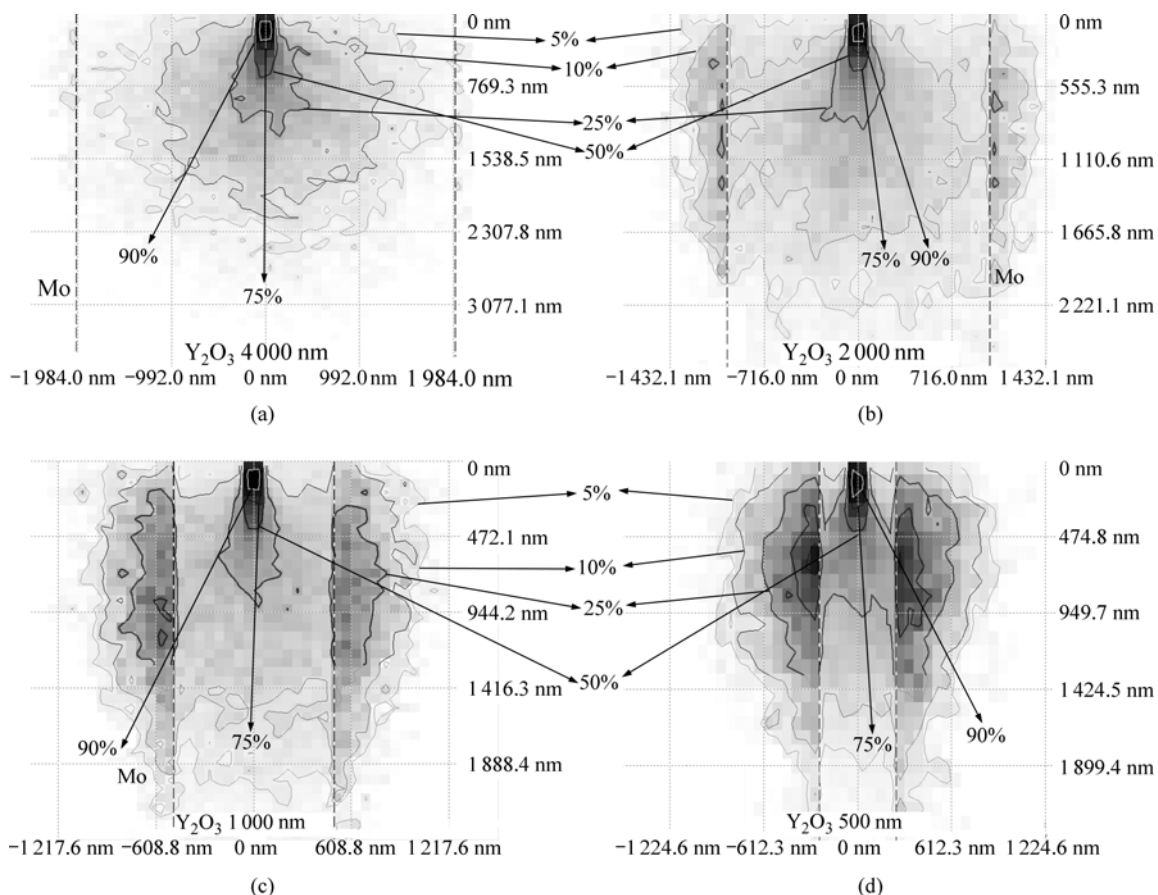


**Fig.4** Electron energy distribution in Mo/ $Y_2O_3$ /Mo structure with different width (Electron bombardment energy of 20 keV)

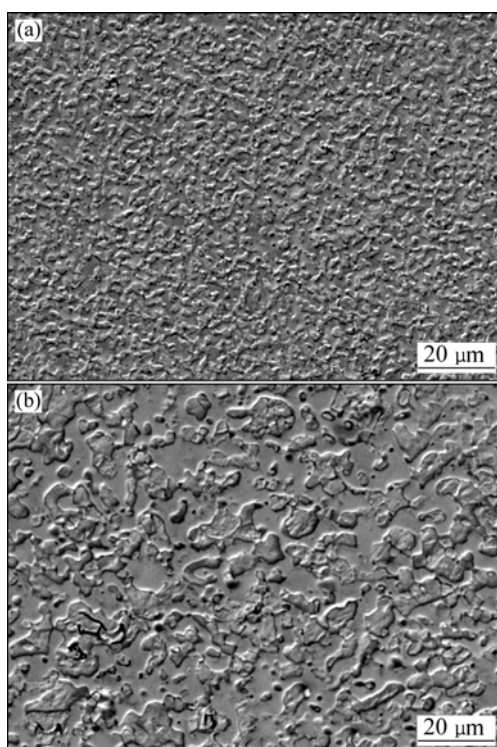


**Fig.5** Back-scattered electron images of  $Y_2O_3$ -Mo emitter prepared by liquid-liquid doping (a) and solid-solid mixing (b)

yield of this emitter is 3.09, far lower than that by liquid-liquid doping method which has fine microstructure. Therefore, the decrease in the grain size of the emitter is favorable for the improvement of secondary emission property.

## 4 Conclusions

1)  $Y_2O_3$ -doped Mo emitter prepared by liquid-liquid doping method has fine microstructure whereas that prepared by mechanical mixing of  $Y_2O_3$  and Mo has large grain size.

2) Two kinds of emissions, reflection emission formed by the secondary electrons produced by primary electrons and transmission emission formed by secondary electrons in  $Y_2O_3$  excited by the internal secondary electrons produced in molybdenum, exist in the emitter with small grain size, while only reflection emission occurs in the emitter with large grain size.

3) The emitter prepared by liquid-liquid doping exhibits better performance in secondary emission, i.e., the highest secondary emission yield of 5.24 could be obtained, which is about 1.7 times that for the emitter

prepared by solid-solid- doping method.

## References

- [1] BISELLO D, CANDELORI A, GIUBILATO P, KAMINSKY A, MATTIAZZO S, NIGRO M, PANTANO D, RANDO R, SILVESTRI L, TESSARO M, WYSS J. Secondary electron yield of Au and  $Al_2O_3$  surfaces from swift heavy ion impact in the 2.5–7.9 MeV/amu energy range [J]. *Nuclear Instruments and Methods in Physics Research B*, 2008, 266(1): 173–180.
- [2] SHIH A, YATER J, HOR C, ABRAMS R. Secondary electron emission studies [J]. *Appl Surf Sci*, 1997, 111: 251–258.
- [3] YERYOMKA V D, KOPOT M A, KULAGIN O P, NAUMENKO V D. Spatial-harmonic magnetrons-THz electromagnetic radiation oscillators [C]// 2008 International Conference on Microwave and Millimeter Wave Technology. Nanjing: Institute of Electrical and Electronics Engineers, 2008: 1199–1201.
- [4] YERYOMKA V D, KOPOT M A, KULAGIN O P. Surface-wave magnetrons: Electromagnetic radiation oscillators in THz range [C]// 16th International Crimean Conference-Microwave and Telecommunication Technology. Crimea: Institute of Electrical and Electronics Engineers, 2006: 265–268.
- [5] THOMAS R E, MORRILL C D. Secondary emission properties of impregnated tungsten cathodes [J]. *Appl Surf Sci*, 1983, 16: 292–311.
- [6] WANG Jin-shu, LI Hong-yi, LIU Juan, WANG Yi-man, ZHOU Mei-ling. A study of secondary electron emission properties of the molybdenum cathode doped with  $RE_2O_3$  [J]. *Appl Surf Sci*, 2003, 215: 273–276.
- [7] WANG Jin-shu, WANG Yi-man, ZHOU Mei-ling. Anti-bombing insensitivity life of molybdenum cathode doped with  $La_2O_3$  and  $Y_2O_3$  [J]. *Mater Sci Eng B*, 2006, 128(1/3): 211–215.
- [8] WANG Jin-shu, LI Hong-yi, YANG Sa, LIU Yan-qin, ZHOU Mei-ling. Study on rare earth oxide-molybdenum cermet cathode materials [J]. *J Alloy Comp*, 2004, 385(1/2): 288–293.
- [9] WANG Jin-shu, LIU Juan, LI Hong-yi. A study on  $La_2O_3$ - $Gd_2O_3$ -Mo secondary emission material [J]. *Transactions of Nonferrous Metals Society of China*, 2003, 13(1): 38–41.
- [10] YANG Sa, ZHOU Mei-ling, WANG Jin-shu. Durability experiment on anti-electron-bombardment of  $RE_2O_3$ -Mo secondary emission material [J]. *Transactions of Nonferrous Metals Society of China*, 2004, 14(2): 274–277.
- [11] DVORKIN V V, DZBANOVSKY N N, SUETIN N V, POLTORATSKY E A, RYCHKOV G S, IL'ICHEV E A, GAVRILOV S A. Secondary electron emission from CVD diamond films [J]. *Diamond & Related Mater*, 2003, 12(12): 2208–2218.
- [12] YOUNG J R. Dissipation of energy by 2.5–10 keV electrons in  $Al_2O_3$  [J]. *J Appl Phys*, 1957, 28: 524–528.
- [13] DEKKER A J. *Advances in research and applications* [M]// SEITZ F, TURNBULL D. *Solid State Physics*. New York: Academic Press, 1958: 251.
- [14] WANG Dao-long, HU Ke-zhi, MA Fu-kang. *Manual for rare metal* [M]. Beijing: Metallurgical Industry Press, 1995: 800. (in Chinese)
- [15] JIANG Jian-ping. *Cathode electronics and theory of gas discharge* [M]. Beijing: National Defense Press, 1980: 205. (in Chinese)

(Edited by YANG Hua)